Current-induced magnetization dynamics in Co/Cu/Co nanopillars

X. Q. Ma,[1,a] Z. H. Xiao,[1] P. P. Wu,[1] J. X. Zhang,[2] S. Q. Shi,[3] and L. Q. Chen[2]
[1]*Department of Physics, University of Science and Technology Beijing, Beijing 100083, China*
[2]*Department of Materials Science and Engineering, The Pennsylvania State University, University Park, Pennsylvania 16802, USA*
[3]*Department of Mechanical Engineering, The Hong Kong Polytechnic University, Hung Hom, Kowloon, Hong Kong*

(Presented on 8 November 2007; received 2 October 2007; accepted 28 November 2007; published online 29 February 2008)

We studied current-induced magnetization dynamics in Co/Cu/Co nanopillars using the Landau-Lifshitz-Gilbert equation incorporating the spin transfer torque effect. We show that the magnetization dynamics can be grouped into four types according to its characteristics and the current density value under zero external field. It is found that an external field can significantly affect the magnetization dynamics, either favoring or impeding the magnetization switching depending on its direction. © *2008 American Institute of Physics*. [DOI: 10.1063/1.2838317]

I. INTRODUCTION

Spin transfer torque[1,2] (STT) results from the angular momentum transfer between two ferromagnets through the electrons in the spin-polarized current flowing through them. If the current density is sufficiently high, spin-wave excitations will be stimulated or even switched the magnetization of a nanoscale magnetic film. The role of STT in magnetization switching and spin-wave excitations has been verified by many experiments.[3–9] In addition to the experimental research, many theoretical studies[10–14] have also been attempted. However, despite extensive studies in this subject, a systematic study on current induced magnetization precession and switching is lacking.

We investigate the magnetization dynamics for a nanoscale pillar structure under the influence of a spin-polarized current with in-plane magnetization traversed by a perpendicular-to-plane current through numerical simulations. The Landau-Lifshitz-Gilbert (LLG) equation including two additional terms that describe the STT effect is employed to model the magnetization dynamics.

II. MODEL AND NUMERICAL SIMULATION

The model geometry of the nanopillar is defined as Co (2 nm)/Cu (4 nm)/Co (10 nm), as shown in Fig. 1. The lateral size of the nanopillar is 64×64 nm^2. With two leads at 8 nm each, the size of the nanopillar is $32\times64\times64$ nm^3. It was divided into $32\times64\times64$ cubic grids. The two Co layers (ferromagnets) are separated by a thin Cu layer (nonferromagnetic metal). The thin and thick Co layers are the free and pinned layers, respectively. As Co possesses uniaxial anisotropy, we assume that the easy axis of both Co layers is parallel to x axis. The free layer magnetization has two stable states in the x orientation, i.e., parallel or antiparallel to positive x axis. The pinned layer magnetization vector $\mathbf{P}$ is fixed at positive x axis, and the initial magnetization vector $\mathbf{M}$ of the free layer is along the same direction. The symmetric in-plane geometry of 64×64 nm^2 is different from most experiments. However, this will not significantly affect our conclusions because the difference between demagnetization fields in the x and y directions in the asymmetric geometry used in the experiment is far smaller than the uniaxial anisotropy field of Co. We adopt the current-perpendicular-to-plane geometry. The positive current is defined as the current flow from the free layer to the pinned layer. The external field is applied only in the x direction.

The modified LLG equation[15] taking into account the STT effect can be written in the form of

$$\frac{d\mathbf{M}}{dt} = -\gamma'\mathbf{M}\times\mathbf{H}_{\text{eff}} - \frac{\alpha\gamma'}{M_s}\mathbf{M}\times(\mathbf{M}\times\mathbf{H}_{\text{eff}}) - \frac{2\mu_B J}{(1+\alpha^2)deM_s^3}g(\mathbf{M},\mathbf{P})\mathbf{M}\times(\mathbf{M}\times\mathbf{P}) + \frac{2\mu_B\alpha J}{(1+\alpha^2)deM_s^2}g(\mathbf{M},\mathbf{P})\mathbf{M}\times\mathbf{P}, \quad (1)$$

where $\mathbf{M}$ is the magnetization vector of free layer, $\gamma' = \gamma/(1+\alpha^2)$, γ is the gyromagnetic ratio, α is the dimensionless damping constant, $\mathbf{H}_{\text{eff}}$ is the effective field, M_s is the saturation magnetization and modulus of magnetization of free layer and pinned layer, μ_B is the Bohr magneton, J is the current density, d is the thickness of the free layer, and e is the modulus of electron charge. The angle between $\mathbf{M}$ and $\mathbf{P}$ is θ, $\mathbf{M}\cdot\mathbf{P}/M_s^2=\cos\theta$. The scalar function $g(\mathbf{M},\mathbf{P})$ was deduced by Slonczewski,[2]

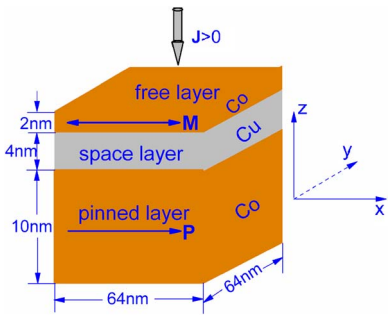

FIG. 1. (Color online) Model geometry definition of Co/Cu/Co nanopillar.

[a]Electronic mail: xqma@sas.ustb.edu.cn.

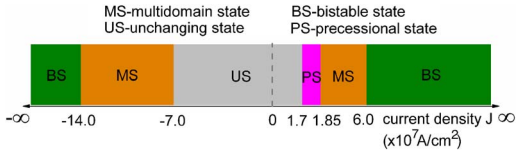

FIG. 2. (Color online) Schematic map of current density range of different magnetization dynamic types. The four different colors correspond to four types of magnetization dynamics. The width of each section represents the current density range of corresponding dynamic type. The missing type of magnetization dynamics for PS to APS is precessional state.

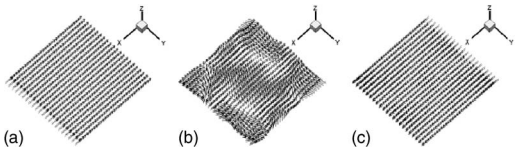

FIG. 3. The domain structure of free layer in different states. (a) The magnetization lies along the $-x$ axis. (b) A multidomain structure of MS under current density of 5.0×10^7 A/cm^2. (c) The magnetization lies along the $+x$ axis.

$$g(\mathbf{M},\mathbf{P}) = [-4 + (1+\eta)^3(3 + \mathbf{M}\cdot\mathbf{P}/M_s^2)/4\eta^{3/2}]^{-1}, \qquad (2)$$

where η is the spin polarizing factor. The first term of modified LLG equation is the precession term that conserves the magnetic energy and determines the precession frequency of the magnetization dynamics. The second term is the damping term that dissipates the energy during magnetization dynamics. The last two terms describe the function of STT, which inclines to drag the magnetization away from its initial stable state and motivates the magnetization precession around effective field, which mainly consist of anisotropy, demagnetization, and exchange field.

We investigated the dynamics of magnetization by numerically solving modified time-dependent LLG equation using the Gauss-Seidel projection method[16,17] with constant time step $\Delta t=0.014\,875$ ps which is small enough to ensure numerical stability and sufficient precision. The detail simulation processes and the parameters used here are same as in Ref. 18.

III. RESULTS AND DISCUSSION

We performed systematic computer simulations of magnetic switching under different current densities. We summarize our results in Fig. 2. Under zero external field, a positive current results in magnetic switching from an antiparallel state (APS) to parallel state (PS) alignment. In this case, the magnetization process can be grouped into four types: unchanging state, steady precessional state, multidomain state, and bistable state. Of the four types, only in the bistable state, the magnetization can be switched back and forth relative to the initial configuration. The competition between STT and the Gilbert damping is dominant for the formation of the four states. On the other hand, a negative current favors APS and leads to magnetic flipping from PS to APS. However, different from the previous case, only three types of states were observed in the reverse process from parallel to antiparallel alignment; the steady precessional state is missing. Under an external field, the magnetization dynamics becomes much more complicated. The critical current density for each state is influenced by the external field which can favors or impedes the magnetization dynamics according to its direction.

Each state in the switching process corresponds to a certain current density range. If current density varies in the range of -7.0×10^7 A/cm^2 $<J<1.7\times10^7$ A/cm^2, the magnetization dynamics lies in the unchanging state. The magnetization does not change and remains in their initial orientation (parallel or antiparallel state). This is the result of the STT energy input being lower than the Gilbert energy dissipation. The magnetization dynamics is heavily damped.

In the range of 1.7×10^7 A/cm^2 $\leqslant J<1.85\times10^7$ A/cm^2, the magnetization lies in the steady precessional state. The magnetic moments precess around the effective field along the x direction, with oscillations at constant frequency and amplitude. The magnetization in free layer is uniform, so it is a single domain. The steady precessional state is reached when the Gilbert energy dissipation equals the STT energy input.

In the ranges of -14.0×10^7 A/cm^2 $<J\leqslant-7.0\times10^7$ A/cm^2 and 1.85×10^7 A/cm^2 $\leqslant J<6.0\times10^7$ A/cm^2, the magnetization lies in the multidomain state. The mechanism of the formation of this state is similar to that of steady precessional state. The differences are that the free layer is not a monodomain, as shown in Fig. 3(b), and that the frequency and amplitude of magnetization oscillation are not constant. The multidomain is formed to reduce the magnetostatic energy. It should be noted that in this state, the magnetization could not be switched by STT either.

When $-\infty<J\leqslant-14.0\times10^7$ A/cm^2 and 6.0×10^7 A/cm^2 $\leqslant J<\infty$, the magnetization dynamics lie in bistable state. In this state, the magnetization can be switched back and forth between two stable states: parallel and antiparallel configurations. The threshold current density from APS to PS is $J_c^{\mathrm{APS}\rightarrow\mathrm{PS}}=6.0\times10^7$ A/cm^2 and that for PS to APS is $J_c^{\mathrm{PS}\rightarrow\mathrm{APS}}=-1.4\times10^8$ A/cm^2. The current density in this state is large enough to switch the magnetization of the free layer, or the STT is always bigger than the Gilbert damping in the whole switching process.

For example, if a magnetization initially was along the $-x$ axis (APS) [Fig. 3(a)], a positive current density greater than 6.0×10^7 A/cm^2 will switch the magnetization to the direction along the $+x$ axis (PS) [Fig. 3(c)]. If the positive current density is smaller than 6.0×10^7 A/cm^2 and greater than 1.85×10^7 A/cm^2, it cannot switch the magnetization, but it leads a multidomain state [Fig. 3(b)]. For the positive current densities between 1.7×10^7 and 1.85×10^7 A/cm^2, it results in a precessional state in which there is no domain switching but with the magnetization presses around its local effective field. For positive current densities smaller than 1.7×10^7 A/cm^2, the initial domain structure will remain unchanged [Fig. 3(a)].

Figure 4 shows the variation of the x component of the magnetization from APS to PS. The characteristics of the two states of multidomain state (MS) and bistable state (BS) in the magnetization dynamics can be obviously seen. The magnetization can be switched only when the current density is large enough, as the curves of $J=-1.5\times10^8$, -2.0×10^8,

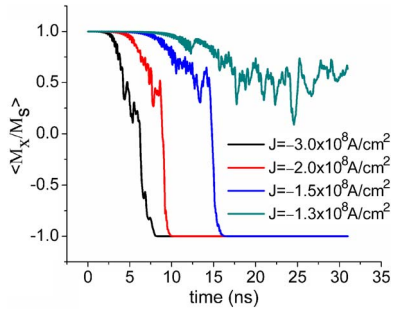

FIG. 4. (Color online) The temporal evolution of the x component of magnetization M_x under four different current densities.

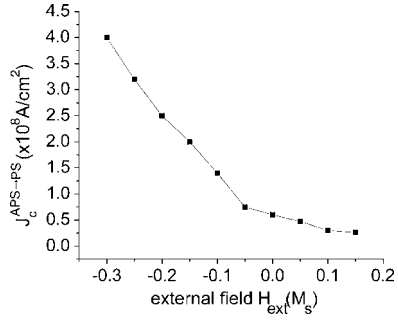

FIG. 6. The relationship of the switching threshold current density vs external field.

and -3.0×10^8 A/cm^2 show, where the magnetization dynamics lie in BS. Otherwise, it cannot be switched as in the case of $J=-1.3\times10^8$ A/cm^2, where the magnetization dynamics lie in MS. It is also obvious that the higher the current density is, the shorter the switching time is.

The magnetization dynamics is more complicated when there is an external field applied along the x direction. Figure 5 shows the magnetization dynamics in current density of 9.0×10^7 A/cm^2 under four different external fields: ie., $0.2M_s$, $0.1M_s$, $0M_s$, and $-0.1M_s$. Through the comparison of four curves, one can find that the external field favors the magnetization switching from antiparallel to parallel alignment when it is in the positive direction and impede the switching in the negative direction. For example, for the current density of 9.0×10^7 A/cm^2, $-0.1M_s$ is large enough to stop the magnetic switching, making magnetization dynamics lie in the multidomain state. When it is in the positive direction, larger external field makes the magnetization switch from APS to PS more quickly.

The magnetization switching threshold is also shown in Fig. 6. When it is in the positive direction, the higher the external field is, the lower the switching threshold current density is. When it is in the negative direction, the higher the external field is, the higher the switching threshold current density is. In fact, the types of magnetization dynamics are mainly decided by the competition between STT and the Gilbert damping.

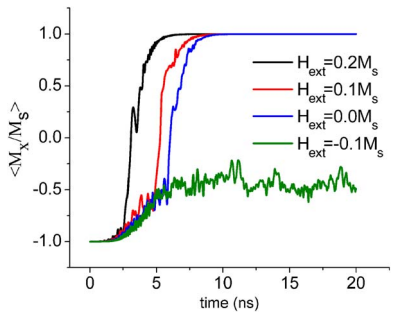

FIG. 5. (Color online) The magnetization dynamics in current density of 9.0×10^7 A/cm^2 under different external fields.

IV. CONCLUSIONS

Based on our systematic computer simulations of current-induced magnetization dynamics in Co/Cu/Co nanopillars, the magnetization process from an APS to PS alignment can be grouped into four types: unchanging state, steady precessional state, multidomain state, and bistable state, depending on the current density. On the other hand, only three types of states, without the steady processional state, were observed in the reverse process from parallel to antiparallel alignment. Under an external field, the magnetization dynamics becomes much more complicated.

ACKNOWLEDGMENTS

This work was supported by the Joint Research Fund for Overseas Distinguished Chinese Young Scholars from the National Science Foundation of China (Grant No. 50428101) and by SRF for ROCS, SEM.

[1] L. Berger, Phys. Rev. B **54**, 9353 (1996).
[2] J. C. Slonczewski, J. Magn. Magn. Mater. **159**, L1 (1996).
[3] E. B. Myers, D. C. Ralph, J. A. Katine, R. N. Louie, and R. A. Buhrman, Science **285**, 867 (1999).
[4] J. A. Katine, F. J. Albert, R. A. Buhrman, E. B. Myers, and D. C. Ralph, Phys. Rev. Lett. **84**, 3149 (2000).
[5] F. J. Albert, N. C. Emley, E. B. Myers, D. C. Ralph, and R. A. Buhrman, Phys. Rev. Lett. **89**, 226802 (2002).
[6] B. Özyilmaz, A. D. Kent, D. Monsma, J. Z. Sun, M. J. Rooks, and R. H. Koch, Phys. Rev. Lett. **91**, 067203 (2003).
[7] M. Tsoi, A. G. M. Jansen, J. Bass, W.-C. Chiang, M. Seck, V. Tsoi, and P. Wyder, Phys. Rev. Lett. **80**, 4281 (1998).
[8] W. H. Rippard, M. R. Pufall, S. Kaka, S. E. Russek, and T. J. Silva, Phys. Rev. Lett. **92**, 027201 (2004).
[9] J. Z. Sun, J. Magn. Magn. Mater. **202**, 157 (1999).
[10] Y. B. Bazaliy, B. A. Jones, and S.-C. Zhang, Phys. Rev. B **57**, R3213 (1998).
[11] J. C. Slonczewski, J. Magn. Magn. Mater. **195**, L261 (1999).
[12] C. Heide, P. E. Zilberman, and R. J. Elliott, Phys. Rev. B **63**, 064424 (2001).
[13] M. D. Stiles and A. Zangwill, J. Appl. Phys. **91**, 6812 (2002); Phys. Rev. B **66**, 014407 (2002).
[14] S. Zhang, P. M. Levy, and A. Fert, Phys. Rev. Lett. **88**, 236601 (2002).
[15] L. Torres, L. Lopez-Diaz, E. Martinez, M. Carpentieri, and G. Finocchio, J. Magn. Magn. Mater. **286**, 381 (2005).
[16] X. P. Wang, C. J. Garcia-Cervera, and W. E, J. Comput. Phys. **171**, 357 (2001).
[17] J. X. Zhang and L. Q. Chen, J. Appl. Phys. **97**, 084313 (2005).
[18] Z. H. Xiao, X. Q. Ma, P. P. Wu, J. X. Zhang, L. Q. Chen, and S. Q. Shi, J. Appl. Phys. **102**, 093907 (2007).